Human Molecular Genetics, 2007, Vol. 16, No. 7 ***763–773***
doi:10.1093/hmg/ddm012
Advance Access published on February 27, 2007

Success and failure in human spermatogenesis as revealed by teratozoospermic RNAs

Adrian E. Platts[1], David J. Dix[3], Hector E. Chemes[4], Kary E. Thompson[3], Robert Goodrich[1], John C. Rockett[3], Vanesa Y. Rawe[5], Silvina Quintana[4], Michael P. Diamond[1], Lillian F. Strader[3] and Stephen A. Krawetz[1,2,6,*]

[1]Department of Obstetrics and Gynecology, [2]Center for Molecular Medicine and Genetics, Wayne State University School of Medicine, USA, [3]Office of Research and Development, U.S. Environmental Protection Agency, USA, [4]Centro de Investigaciones Endocrinologicas, Argentina, [5]Centro de Estudios en Ginecología y Reproducción, Argentina and [6]Institute for Scientific Computing, Wayne State University

Received December 29, 2006; Revised January 26, 2006; Accepted February 2, 2007

We are coming to appreciate that at fertilization human spermatozoa deliver the paternal genome alongside a suite of structures, proteins and RNAs. Although the role of some of the structures and proteins as requisite elements for early human development has been established, the function of the sperm-delivered RNAs remains a point for discussion. The presence of RNAs in transcriptionally quiescent spermatozoa can only be derived from transcription that precedes late spermiogenesis. A cross-platform microarray strategy was used to assess the profile of human spermatozoal transcripts from fertile males who had fathered at least one child compared to teratozoospermic individuals. Unsupervised clustering of the data followed by pathway and ontological analysis revealed the transcriptional perturbation common to the affected individuals. Transcripts encoding components of various cellular remodeling pathways, such as the ubiquitin–proteosome pathway, were severely disrupted. The origin of the perturbation could be traced as far back as the pachytene stage of spermatogenesis. It is anticipated that this diagnostic strategy will prove valuable for understanding male factor infertility.

INTRODUCTION

At fertilization, a spermatozoon brings to the nascent embryo the haploid paternal genome, a complement of proteins and a group of paternally transcribed RNAs (1–3). These paternal transcripts include a subset of functionally viable full-length mRNAs (4). Discussion continues as to the extent to which these RNAs are part of the complex prerequisite for successful embryogenesis and placentation. Evidence for these RNAs regulating development and sperm maintenance during sperm transport within the female reproductive tract continues to accumulate (5,6). Irrespective of their role, spermatozoal RNAs have the potential to provide a window into the fidelity of male gametogenesis.

The WHO (7) and Kruger's strict criteria (8) are the two primary schemes employed to classify spermatozoa. They differ in both the parameters measured and the percentage of spermatozoa of ideal morphology required, 30 and 14%, respectively, to classify a specimen as 'normal'. Teratozoospermic morphologies vary widely. The most common form is described by heterogeneous sperm anomalies of acquired origin secondary to other conditions affecting the reproductive system. In comparison, there are other forms with familial clustering and presumed genetic origin that display a relatively homogeneous sperm phenotype. These include acephalic spermatozoa, round-headed acrosomeless spermatozoa, acrosomal hypoplasia, dysplasia of the fibrous sheath (DFS) or stump tail defect and the dynein-deficient axonemes of the 'immotile cilia syndrome' (9). The likelihood of successful conception for individuals demonstrating the most severe levels of teratozoospermia is reduced. Although diagnosis of most forms of teratozoospermia is straightforward, there are borderline instances and those of the idiopathic infertile male where diagnosis and understanding its origins are hindered by the subjective methods that are routinely employed to identify and classify these anomalies.

*To whom correspondence should be addressed at: Charlotte B. Failing Professor of Fetal Therapy and Diagnosis, 253 C.S. Mott Center, 275 East Hancoc, Detroit, MI 48201, USA. Tel: +1 3135776770; Fax: +1 31357-8554; Email: steve@compbio.med.wayne.edu

Spermatozoal RNAs represent an untapped diagnostic resource with the potential for discriminating among the highly variable clinical manifestations of disrupted and/or aberrant spermatogenesis. This could alleviate some of the uncertainties in assessing the cause of an individual's infertility. To test this notion, we have examined the complement of transcripts characteristic of a well-characterized pathology, human teratozoospermia. Using a high-throughput microarray-based strategy, we describe a disrupted pathway common to a range of teratozoospermic presentations.

RESULTS

The severity of teratozoospermia is generally characterized through microscopic observation using the WHO or the Kruger strict criteria. These provide a reasonably effective manner to identify the affected individuals but has yet to address the underlying etiology. Recently, electron microscopy and immunostaining have been employed to describe the primary structural perturbations that contribute to this pathology (9). These include the failure of sperm nuclear chromatin to fully condense into its protamine-bound state, unusual or incomplete development of the acrosome, disorders of head–tail attachment with abaxial tail implantation, acephalic spermatozoa and various forms of dysplastic development of the sperm tail cytoskeleton and mitochondrial sheath such as the DFS/stump tail syndrome. Although these approaches have proven fruitful, we still do not understand how and whether these various manifestations are connected by a common pathway. The results presented below describe a genome-wide survey that begins to delineate these pathways and demonstrates the utility of a new diagnostic paradigm.

Eight semen samples were provided from patients who presented with severe and consistent teratozoospermia, T_z, using the strict criterion of percent ideal form (PIF) that $\leq 3\%$ of spermatozoa displayed the ideal form. This rigorous criterion relative to Kruger's guideline of 4% PIF (10) was selected since this class exhibits a very poor prognosis of fertility (11). To disaggregate confounding syndromes, only those individuals presenting as teratozoospermic with normal sperm motility and concentration and no other severe pathologies were initially selected. Representative photomicrographs of the T_z samples are shown in Figure 1. These include examples of several teratozoospermic phenotypes. This group of samples presented a host of aberrations and was classified as generally representing non-systematic teratozoospermia or heterogeneous teratozoospermia, the most common form. Semen samples were also collected from a control group of 13 reproductively normal, N_s, males who had fathered at least one child. Their semen characteristics are summarized in Table 1. As expected, the PIF score clearly separated the N_s from the T_z group. The N_s group displayed a broader range of characteristics, typical of the fertile human male.

To assess whether the distribution of spermatozoal RNAs could be used to predict clinical diagnoses, transcript profiles were subjected to unsupervised hierarchical clustering. As shown in Figure 2A, all 21 samples were clustered in full accordance with their diagnosis. This was irrespective of the microarray platform, i.e. Affymetrix or Illumina or data normalization or modeling strategy employed using BeadStudio, RMA or DChip.

As shown in Figure 2B, applying the rigorous criterion of a ten-fold change ($P < 0.001$) prior to hierarchical gene clustering revealed with very high confidence a set of transcripts capable of highlighting the spermatogenic disruption. Principal component analysis (PCA), shown in Figure 2C, of this set of transcripts reiterated the linear separability of the N_s and T_Z samples into two clinically distinct groups. To assess the power of this classification approach, we examined an additional set of samples collected at a third site that were presented in a blind manner. Their semen characteristics are summarized in Table 2 and a representative physical summary is presented in Figure 3A. These T_z samples showed extremely low PIF values. The majority, samples 23A–23E, displayed a predominance of short, thick, irregular tails. Among the DFS samples, at least 75% and up to 100% (median 96%) of the spermatozoa were classified as having a dysplasia of the fibrous sheath. The last sample, 23F, corresponded to typical globozoospermia with higher than 90% round-headed acrosomeless spermatozoa. Both DFS and globozoospermia display very well characterized, homogenous sperm phenotypes (9).

The clustering of these samples was determined using 286 well-characterized human RefSeq genes present on the Illumina WG8 array platform. These represent a subset of the 439 transcripts previously identified as differentially abundant between the N_s and T_z groups (Fig. 2Ai) on the WG6 arrays that surveyed both the well-characterized RefSeq genes and the gene candidates. As shown in Figure 3B, using the previously defined 286 transcript diagnostic subset, class assignment of this independent set of samples clearly partitioned the N_s and T_z into two distinct groups ($P \leq 0.015$).

Ontological and pathway mapping of the differentially abundant transcripts from both the Illumina and Affymetrix platforms were concordant when analyzed using three independent systems: NIH DAVID 2.1, Ariadne Genomics Pathway Studio and Genomatix Bibliosphere (12–14). This revealed that in the T_z group, proteosomal RNAs associated with the ubiquitin–proteasomal pathway (UPP) were almost completely suppressed in a pattern similar to that reported in the aging rat model (15) as well as in animals exposed to theophylline or 1,3-dinitrobenzene (16). The proteasome is a large 26S multicatalytic protease typically composed of a barrel-shaped 20S catalytic core capped on one or both ends with a 19S regulatory subunit or an 11S activator complex (17). This forms the non-lysosomal degradative machinery of eukaryotic cells (18). Polyubiquitinated proteins are typically docked to the 19S cap where they are deubiquitinated and then transported to the lumen of the 20S core in which the substrate protein is cleaved into small peptides. As summarized in Figure 4, and detailed in Supplementary Material, Table S1, the UPP was broadly disrupted in T_z, whereas other pathways such as the lysosomal system were unchanged. The transcripts corresponding to the various constituents of the ubiquitin elements of the UPP displayed a non-uniform pattern of changes reflective of their diverse roles in selectively tagging specific subsets of proteins for removal. Transcripts corresponding to the proteasomal components of the UPP exhibited a coordinately regulated suppression reflective of its multi-component structure.

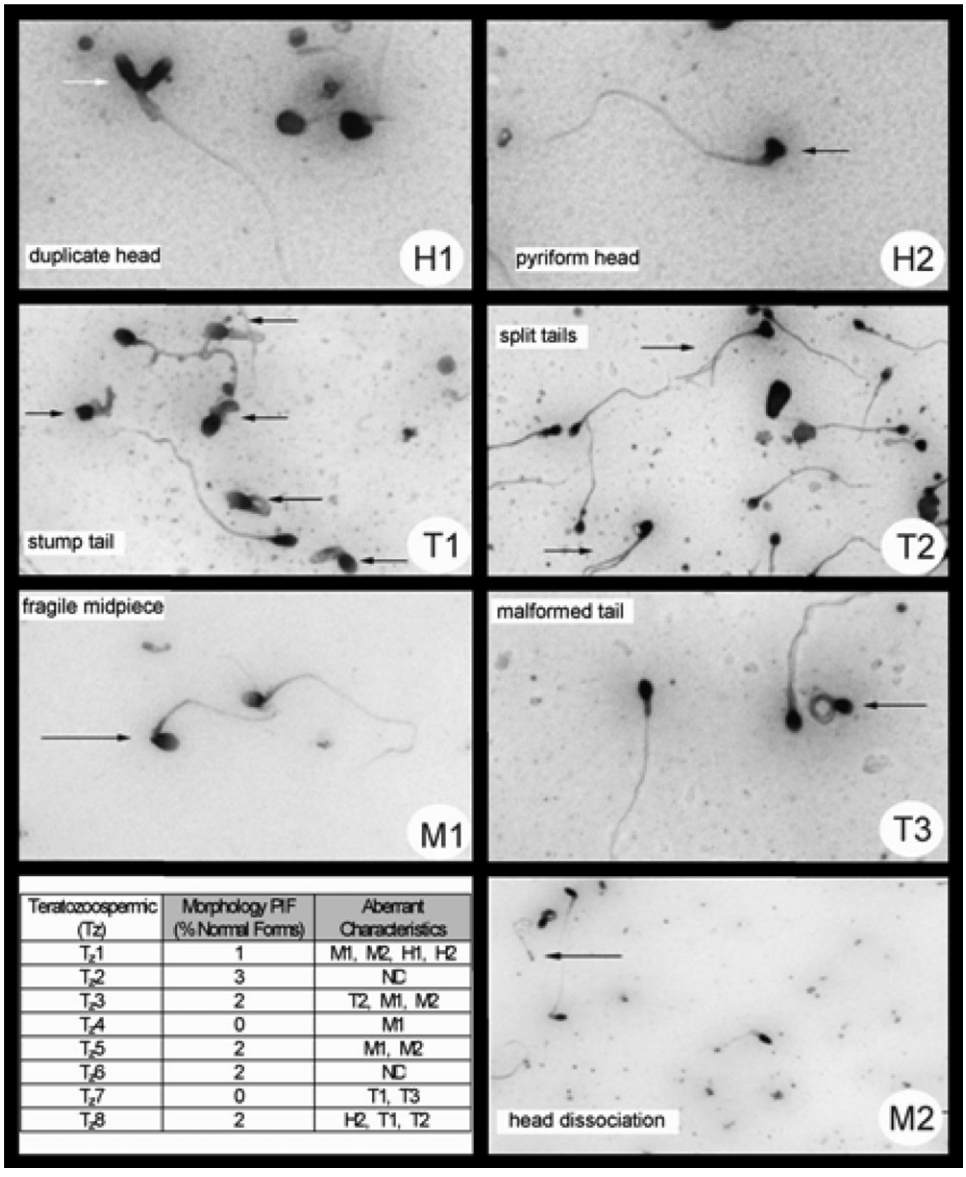

Teratozoospermic (Tz)	Morphology PIF (% Normal Forms)	Aberrant Characteristics
T_z1	1	M1, M2, H1, H2
T_z2	3	NC
T_z3	2	T2, M1, M2
T_z4	0	M1
T_z5	2	M1, M2
T_z6	2	NC
T_z7	0	T1, T3
T_z8	2	H2, T1, T2

Figure 1. Teratozoospermic morphology. The percentage normal sperm morphologies are indicated for the single semen samples assessed in the T_z, teratozoospermic group. The T_z samples are further related to the major location of their structural disruption, head (H), mid-piece (M) or tail (T) and several frequent subphenotypes are illustrated at a magnification of 200× indicating the heterogeneity of presentation.

The ATP-driven UPP degradation pathway includes over 30 ubiquitin conjugating enzymes and ubiquitin ligases (19). This pathway has long been recognized as a key to the successful morphological progression of spermiogenesis (20–22). Ubiquitin acts to tag proteins for proteasomal degradation through a process that is moderated by a plethora of de-ubiquitinylating proteases. The interaction between surface-expressed ubiquitins in the neck region and the acrosome of morphologically abnormal spermatozoa may target incompetent spermatozoa for further ubiquitination by epididymal E3 ligases in preparation for phagocytosis (23,24). This could either reflect tagging that has been carried forward from the meiotic phase that employs apoptosis for germ-cell quality control or post-meiotically, as proteins are degraded during flagellum development.

The majority of the protein-group-specific E2 conjugating protein transcripts were significantly depressed, whereas the E1 ubiquitin-activating enzyme transcripts were somewhat under-represented in T_z. Specifically, RNAs for the large group of E2D proteins were up to 14-fold less abundant as were the transcripts for the E2N conjugating enzymes. Among the E3 ligases, the HECT-type ligase RNAs encoding proteins with both C2 and WW domains were generally more abundant in T_z spermatozoa as were the E2W, E2A and E2E3 conjugating protein RNAs. In contrast, the remaining E3 ligase RNAs were generally under-represented. For example, of the eight reporters for E3A, all were reduced up to 10-fold in the T_z samples. Interestingly, the interaction of the E3A ligase with the human Y domain specific gene *BPY2* (*VCY2*), a protein product that localizes to germ cell

Table 1. WHO 1999 spermatogenic semen parameters from N_s and T_z sample groups

	Volume (ml)	Concentration ($\times 10^6$/ml)	Morphology (PIF)	Motility (%)
N_S				
N1	2.0	24	22	33
N2	3.4	30	6	27
N3	1.0	185	14	40
N4	3.3	164	19	22
N5	6.7	57	27	47
N6	3.4	60	12	44
N7	1.2	175	16	6
N8	1.8	67	25	37
N9	3.7	33	23	34
N10	1.3	209	17	37
N11	2.4	47	12	0.6
N12	1.9	44	15	23
N13	1.5	25	9	33
T_Z				
T1	4.3	50	1	44
T2	3.8	22	3	75
T3	4.5	62	2	60
T4	3.8	34	0	49
T5	5.3	80	2	58
T6	7.3	63	2	50
T7	3.5	44	0	62
T8	4.8	60	2	60

Samples from the N_s group were from subjects who ranged in age from 28 to 39 with a median age of 34 years, T_z age range was 21–40 with a median age of 31 years. All measures of appearance and pH were within the normal range for both groups. Cell contamination ranged from <1 to 7% with a median of less than 3% of the total number of cells. A consistent teratozoospermic phenotype was observed at each of two collections of T_z. The average is presented. Motility of T_z samples was assessed manually. N_s individuals were from normally reproductive subjects having successfully fathered at least a single child. Motility of N_s samples was assessed by computer-assisted sperm analysis.

nuclei, has been shown to be required for normospermia (25,26).

Forks in the ubiquitinylation pathway provide access to alternative protein-specific degradative pathways. The depletion of T_z transcripts may directly lead to the path of reduced protein biosynthesis and thereby reduce cellular remodeling. This failure in spermiogenesis could lead to ubiquitin-linked necrotic and apoptotic pathways (21) becoming activated, as indicated by the elevation of multiple reporters for the apoptotic pathway in T_z, including *INSR*, *CASP1* and *CASP8*, *BIAP1*, *WWP2*, *RERE* and several members of the MAP kinase signaling pathway. These strong linkages between the pathology and differences in sperm RNA content permitted effective classification of the T_z and N_s samples based solely on hierarchical clustering of the ubiquitin and ubiquitin-linked transcripts.

If spermatozoal transcripts provide a record of past events, then they offer a window into the likely developmental and differentiative stages when spermatogenic gene expression was altered. Murine spermatogenesis was used as a proxy to identify subgroups of at least 100 transcripts that initiate and end their peak expression in specific germ cell types during spermatogenesis. Their human orthologs (27) were then linked to each cell type and spermatogenic stage. A compound profile with significant differences between N_s and T_z groups is shown in Figure 5. There is a marked reduction of pachytene spermatocyte associated transcripts and to a lesser extent spermatid-associated transcripts in T_z affected individuals. Interestingly, spermatogonial transcripts like *NUMA1* were equivalent in N_s and T_z samples. This supports the view that disruption of spermatogenesis reached as far back as the pachytene spermatocyte stage. Examples of post-spermatogonial disruption include *HSPA2* ($P \simeq 0.001$) transcribed in spermatocytes and genes for the structural proteins of the flagellum transcribed in spermatids.

DISCUSSION

The lack of both spermatocyte and spermatid transcripts in T_z affected individuals characterized by 134 reporters shown in Supplementary Material, Table S2, is indicative of the failure of late-stage spermatogenesis. This was exemplified by the loss of *HSPA2* that is associated with morphologically disrupted and apoptotic spermatozoa (28). The reduction in *HSPA2* mRNA that encodes a chaperone protein responsible for chromosome desynapsis and reconfiguring the sperm plasma membrane was resonant with up to 7-fold depletion of *ODF 1–4* mRNAs that encode four of the non-tubulin components of sperm tails (29) and acrosomal proteins *ACRV1* and *SPAM1*. In addition to the UPP family, protein phosphatases such as *CDKN3*, *DUSP13*, *PPM1B*, *PPP1* and myosin phosphatase were also generally identified by ontology and pathway analysis as disrupted along with transcripts encoding elements associated with centrosomal reduction in late spermatid development (21). Our understanding of the role of these differentially abundant late-stage transcripts for the most part must await their biological characterization in the spermatogenic context.

The distribution of proteasomes within a cell has been shown to essentially mirror the distribution of ubiquitins. Clusters are present around the distal centriole complex (9) and the acrosome region in maturing spermatozoa. Proteasomal transcripts were broadly and virtually without exception under-represented in T_z, contrasting the relatively complex disrupted fingerprint of the ubiquitin transcripts. RNAs corresponding to the majority of the proteins mapped to the proteasome in KEGG (30) were negatively disrupted by more than 5-fold and by up to 21-fold in T_z. Changes in the ratio of constitutive and inducible proteasomal core subunits of inducible PSMB1, PSMB5 and PSMB7 relative to PSMB8, PSMB9 and PSMB10 were examined. This ratio was 2:1 in N_s and 3:1 in T_z, suggesting that the proteasome is not necessarily assuming a different function in the T_z samples.

The cessation of transcription during chromatin compaction, as well as the disappearance of numerous spermatid organelles, creates challenges throughout spermation and epididymal maturation. The data reported above are concordant with the evidence observed for arrested development in teratozoospermia (9). The gross incapacity of the germ cell to adequately differentiate can be linked to a cycle of synthesis and degradation that inherently includes the UPP. In such a resource-restricted environment, the cell might require targeted autophagy (31,32) with proteosomal degradation facilitating the scavenging of amino acids and other components for

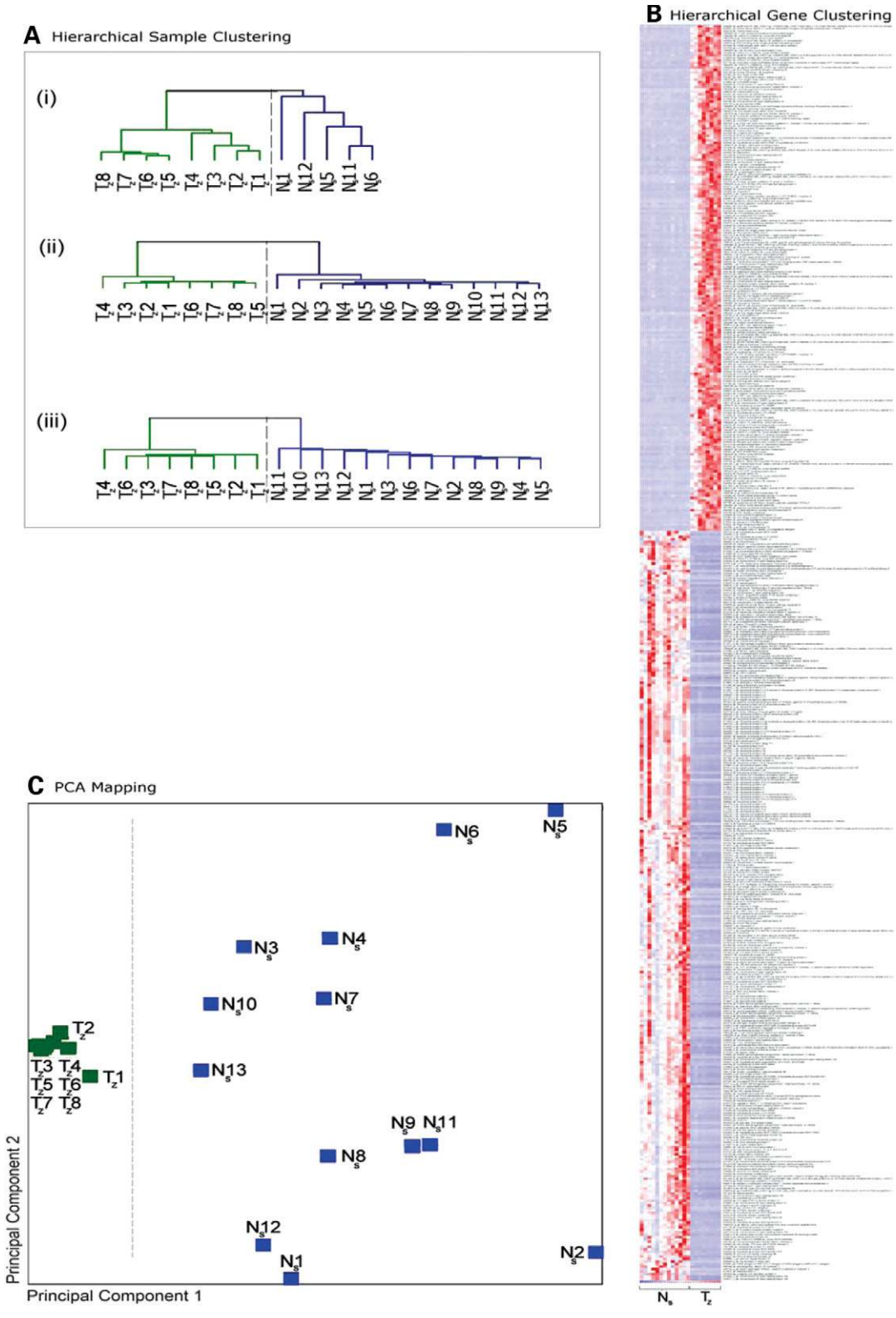

Figure 2. Clustering of transcript abundance profiles from teratozoospermic, T_z, and normospermic, N_s, spermatozoa. (**A**) Unsupervised hierarchical clustering of transcript abundance in T_z (green) and N_s (blue) groups using correlation as the distance metric to cluster samples from (i) the Illumina Sentrix WG-6 platform using BeadStudio (ii) DChip interpretation of the Affymetrix U133 version 2 platform and (iii) the Affymetrix U133 version 2 platform with RMA used for signal quantification. (**B**) Clustering the 516 most differentially abundant transcripts (fold change ≥ 10, $P \leq 0.001$) clearly partitions to T_z and N_s spermatozoal RNAs. This revealed several ontological and affected pathways. (**C**) Combining signals from this subgroup of 516 differentially expressed genes into a PCA model shows immediate linear separability of T_z (green) from N_s (blue) fully concordant with their clinical pathology.

Table 2. Test samples

	DFS (%)	Volume (ml)	Concentration ($\times 10^6$/ml)	Morphology (PIF)	Motility (%)
N_S					
N19-B	0	2.5	250	18	65
N19-C	0	6.0	150	25	50
N23-G	0	4.2	200	23	70
N23-H	0	3.2	180	17	50
T_z					
T23-A	100	2.8	7.2	0	0
T23-B	100	2.0	28	0	0
T23-C	75	3.5	34	3	0
T23-D	90	5.4	6	0	0
T23-E	96	2.4	10.5	0	0
T23-F	0	3.0	12	0	2

WHO 1999 spermatogenic semen parameters from N_s and T_z sample groups. Sample from the N_s group were from subjects that ranged in age from 37 to 57 with a median age of 44 years, T_z age range was 29–42 with a median age of 36 years. All measures of appearance and pH were within the normal range for both groups. Cell contamination was negligible. Motility was assessed manually and is the sum of rapid and slow movement. N_s individuals were from normally reproductive subjects having successfully fathered at least a single child. Motility is described as percentage of rapid and slow movement sperm. The percentage of DFS spermatozoa in each sample is indicated.

de novo protein synthesis. Proteasomes would be required proximate to sites of cellular transformation including the connecting piece of the spermatozoa (33) as well as around the acrosomal cap. A diminution of proteasomal mRNAs, although perhaps not sufficient to halt spermatogenesis, would inhibit morphogenesis by impeding the positioning of the acromosomal cap, sperm nuclear condensation and sperm tail and mid-piece maturation. This would have consequences for the capacity of even motile spermatozoa to initiate fertilization. In the absence of a fully competent acrosome structure, sperm–oocyte penetration would be greatly impaired and intracytoplasmic sperm injection indicated.

As a proof of principle for the utility of a microarray-based spermatozoal RNA assay for determining male factor fertility status, we have shown that RNA fingerprints from normospermic and teratozoospermic semen samples are substantially different. This included both non-systematic teratozoospermia and DFS. The difference was of a sufficient magnitude to enable a diagnostically accurate categorization on the basis of transcript abundance in various ontological subgroups or from the entire transcriptional profile. Diagnostic accuracy was achieved irrespective of the microarray platform or analytical protocol employed and is thus likely to be of sufficient sensitivity to distinguish between cases where prior resolution based on the current standard has not afforded diagnosis. This is clearly shown by the data presented in Figure 3B. The group of samples classified as >90% DFS clustered away from the globozoospermia sample used as an outlier along with a sample characterized by only 75% DFS. This is in accord with the view that this platform strategy may resolve the severity of DFS. Its application to defining the various forms of what is now known as idiopathic male factor infertility is clear.

Transcript profiling identified the UPP as the major cellular system that was disrupted in T_z samples and was concordant with the known disruption of these processes and the subsequent abnormal development of teratozoospermia (9). This was mirrored by an increase in mRNAs associated with apoptotic decay. Both were revealed by employing a general transcriptional survey technique that, unlike highly focused studies, facilitates both targeted analysis and discovery alike. These dual qualities are essential when evaluating idiopathic male infertility. Perhaps the clinical implementation of this strategy will resolve the origins and mechanism. Collectively, this has provided firm ground for the development of a non-invasive diagnostic test capable of revealing the detailed molecular genetics of male infertility. This new strategy takes us from the phenomenological approaches that largely fail to uncover the underlying causes of infertility to an objective measure of the molecular pathway(s) that can reveal its etiology. Ultimately, this approach could lead the clinician to the physiological, environmental or genetic origins of the perturbation and thus used to direct treatment as personalized medicine emerges.

MATERIALS AND METHODS

Sample collection and RNA isolation and probe labeling

Human ejaculates were collected by masturbation from 17 normal fertile men and 14 teratozoospermic men aged 21–57, following IRB protocols H-06-67-96 and HIC 095701MP2F at Wayne State University and IRB protocol 32-EPA-223 at EPA's Human Studies Division in Chapel Hill, NC. Samples were also obtained from Centro de Investigaciones Endocrinologicas and Centro de Estudios en Ginecología y Reproducción, Argentina. Men participating in this study gave informed consent to use their semen for research. Normal male fertility was defined by the ability to father a child by natural conception, whereas teratozoospermia used the strict criterion that ≤3% of spermatozoa displayed PIF. As part of standard Andrology laboratory practices, this was determined either using CASA or by manual evaluation in a site protocol dependent manner. The semen was liquefied for at least 30 min, then washed in somatic cell lysis buffer (0.1% SDS, 0.5% Triton X-100 in dH_2O). This method

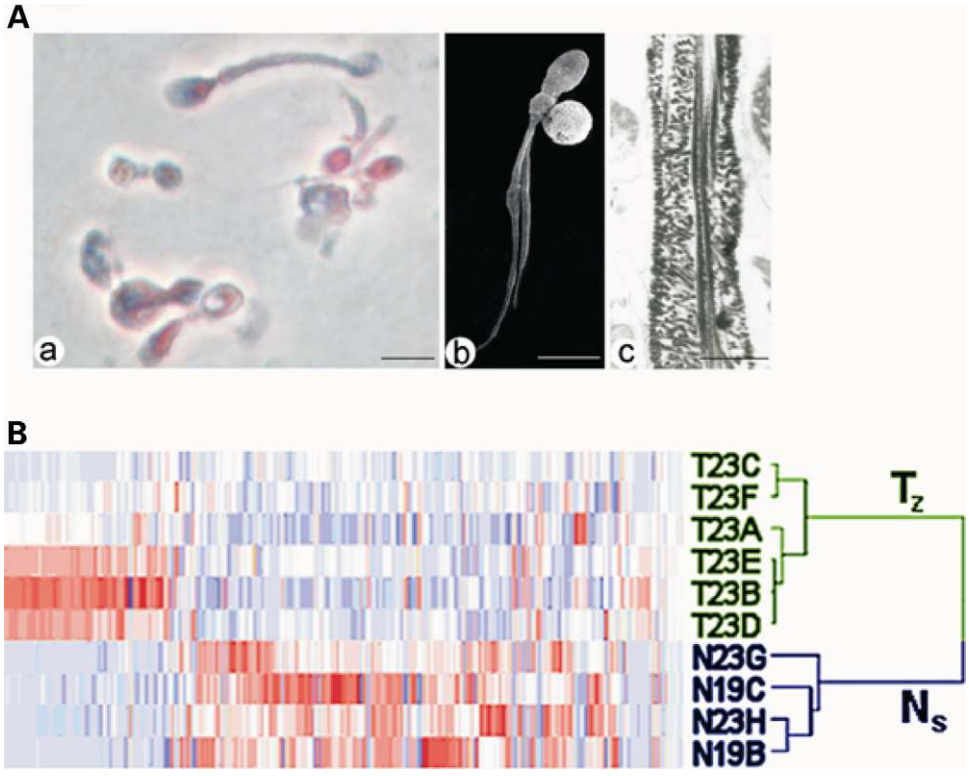

Figure 3. Characterization of DFS spermatozoa and transcript clustering. (**A**) microscopic evaluation of DFS. (a) Phase contrast microscopy of short, thick and irregular tails in DFS spermatozoa. (b) Scanning electron micrograph of DFS spermatozoa with duplicated, short and thick tails. (c) Longitudinal section through the principal piece of a human DFS flagellum. The hyperplasia and disorganization of the FS components is evident. Scale bars correspond to 5 μm for (a) and (b) and 1 μm for (c). (**B**) Hierarchical clustering of an independent sample set. Genes previously identified as differentially abundant between the N_s and T_z groups (fold change ≥ 2, *t*-test $P < 0.01$) were used to cluster the class assignment of an independent set of samples. The samples showed a bimodal cluster on the Illumina platform using the 286 diagnostic gene set in accordance with their clinically ascribed N_s or T_z phenotype.

produces an essentially pure population of spermatozoa that have been shown to be devoid of residual bodies and depleted of somatic cells (1). RNA was then placed in a chaotropic solution for immediate processing or could be stored in this solution for several weeks at room temperature. If long-term storage was required (Wayne State University), the samples were not immediately subject to somatic cell lysis but placed in frozen storage buffer (FSB; 50 mM HEPES buffer, pH 7.5, 10 mM NaCl, 5 mM Mg-acetate and 25% glycerol) then stored at -80°C. The samples were thawed as required, then washed twice in an excess of PBS prior to somatic cell lysis. RNA was then isolated essentially as described (1,34). The RNA thus isolated was then amplified and probes prepared according to manufacture's instructions (Message Amp II, Ambion). Prior to hybridization, probe quality was verified using an Agilent BioAnalyzer. Equal amounts of quality probe were then hybridized to the Affymetrix U133 version 2 arrays or the Illumina Sentrix WG-6/8 bead chip arrays.

Microarray quantification

Transcript profiles from both teratozoospermic, T_z, and normospermic, N_s, semen samples were assessed (NCBI GEO: GSE6969) on the short-oligonucleotide-based Affymetrix U133 (version 2) microarrays (35) with ~54,000 reporters and/or against profiles measured on the technologically distinct Illumina Sentrix WG6 platform with ~46,000 reporters and WG8 with ~24,000 reporters (36). The characteristics of the Illumina Sentrix WG BeadChip platform were independently evaluated (37). Technical replicates demonstrated a high level of reproducibility with an $r^2 = \sim 0.998$. All samples hierarchically clustered to their replicates with $P < 0.01$. To minimize algorithmic artifacts, Affymetrix U133 version 2 data were quantified independently with GCOS 1.1 [MAS 5 algorithm (38)], DChip [MBEI algorithm employing invariant set normalization and modeling in PM-MM mode (39)], Genomatix ChipInspector [SAM algorithm (40)] and R/Bioconductor [RMA procedure: JustRMA (41). For brevity, expression on Affymetrix U133 version 2 arrays quantified by DChip is presented. This approach consistently detected 8,293 reporters in N_s and 7,227 in T_z, of which 4,849 were common to both groups. To identify those transcripts that clearly partitioned between the N_s and T_z samples, a variance profile was constructed for each transcript relative to the group's mean signal for that transcript. Of all the N_s transcripts, 96.5 − 98.5% were observed within 5-fold of the cluster mean signal ($0.82 < r^2 < 0.95$; single outlier of 0.62 omitted) and similarly 97.5% of the T_z transcripts were within 5-fold of the cluster mean signal ($0.64 < r^2 < 0.91$). These ranges may reflect lifestyle variables among the biological replicates that were not rigorously controlled. *A priori*

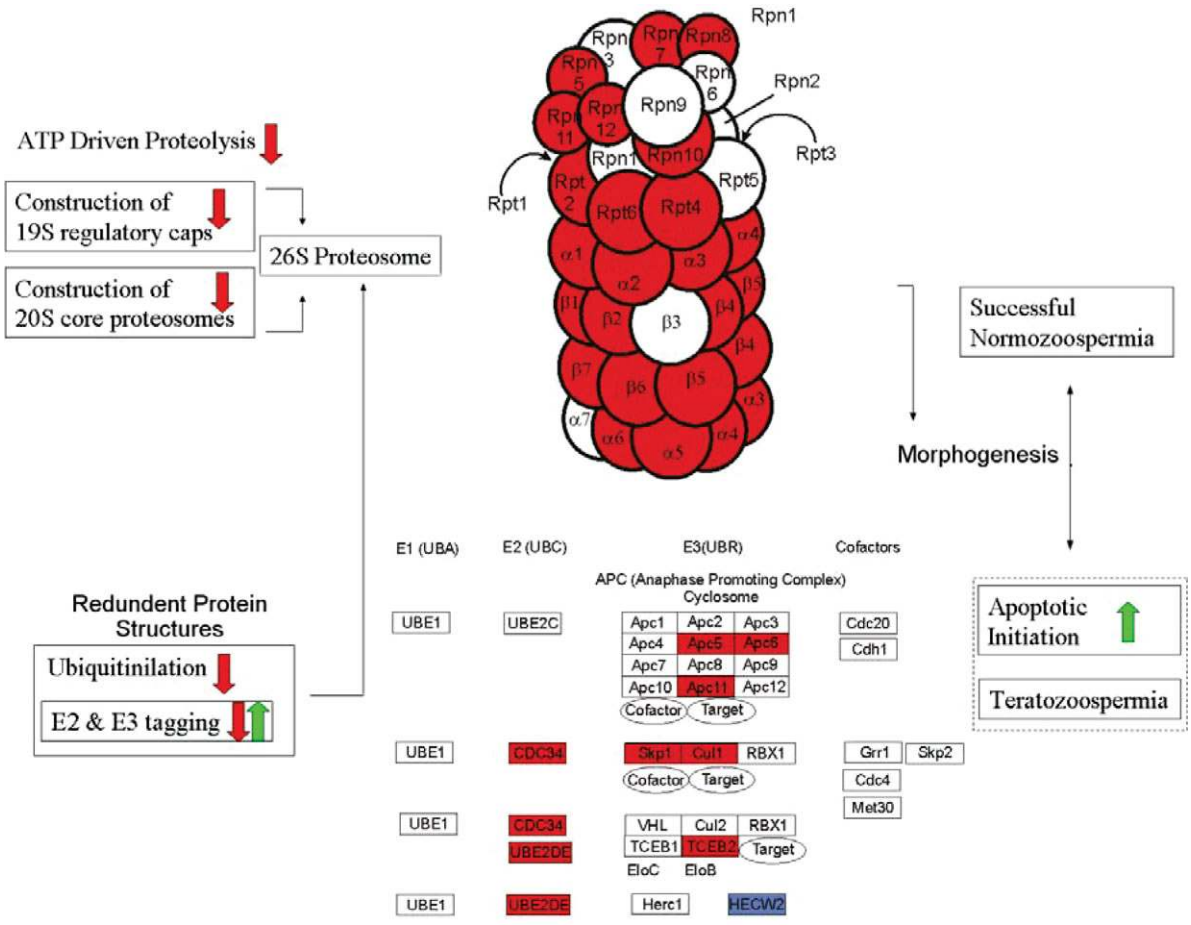

Figure 4. Teratozoospermic pathway. Subcellular systems displaying gross differential changes in the levels of transcripts in normospermic N_s and teratozoospermic T_z samples of at least a 5-fold change at $P < 0.01$ are illustrated. Groups of transcripts that decreased in abundance in teratozoospermia are indicated by red arrows and those that increased by green arrows. Depleted transcripts of systems mapped by KEGG are indicated as red colored structures, blue coloring denotes a super-abundance.

variance models and power estimates (42) were employed to determine the power of the approach. These were then adjusted *post hoc* to understand the reported signal. Variance was hypothesized to arise from three sources, instrument (microarray), preparation (contamination) and subject (biological). Affymetrix and Illumina microarray variance of technical replicates r^2 $\simeq$0.98–0.99 were typical. Seeking an experimental power in excess of 0.8 with a low false discovery rate (FDR), using a minimum of eight arrays in the two groups, an $\alpha \leq 0.001$ in conjunction with $\Delta \geq 10$-fold was suggested. A *post hoc* analysis was conducted to assess the extent to which the *a priori* FDR had been achieved. This was assessed through a Westfall and Young permutation to the sample classification conducted 500 times. The randomized sample sets were assessed in the same way as the original data set and the median FDR was noted. *Post hoc* analysis of signal variance indicated that this was overly conservative and thresholds could be reduced to $\alpha \leq 0.01$ with $\Delta \geq 5$-fold. The experimental power was thereby increased above 0.98. Such an approach might, however, result in an unacceptably high false discovery rate. The FDR was investigated through sample permutation that in turn suggested that the FDR remained much lower, and hence the effect size was likely larger than that had been assumed (mean 1E − 5). A 5-fold difference in signal levels at a confidence of $P < 0.01$ was thus used to generate lists of genes to be included in both ontological and pathway clustering. Sample preparation variance in the above was assumed to be unbiased. Illumina Sentrix WG6 data were analyzed using the rank invariant normalization mode of Illumina BeadStudio (43). Similarly, a 5-fold change in signal in conjunction with a $P < 0.01$ confidence was adopted to generate lists of differentially abundant genes. Tables that contain the complete list of differentially abundant (Supplementary Material, Table S3) and similarly abundant (Supplementary Material, Table S4) transcripts identified on the Affymetrix platform are available as part of the Supplementary Material. Owing to the extent of the profile differences between T_z and N_s samples, possible residual error in normalizing the T_z relative to the N_s samples was explored. Genes were ranked according to their mean expression in the two data sets. Genes with the greatest rank change between the two data sets were noted and

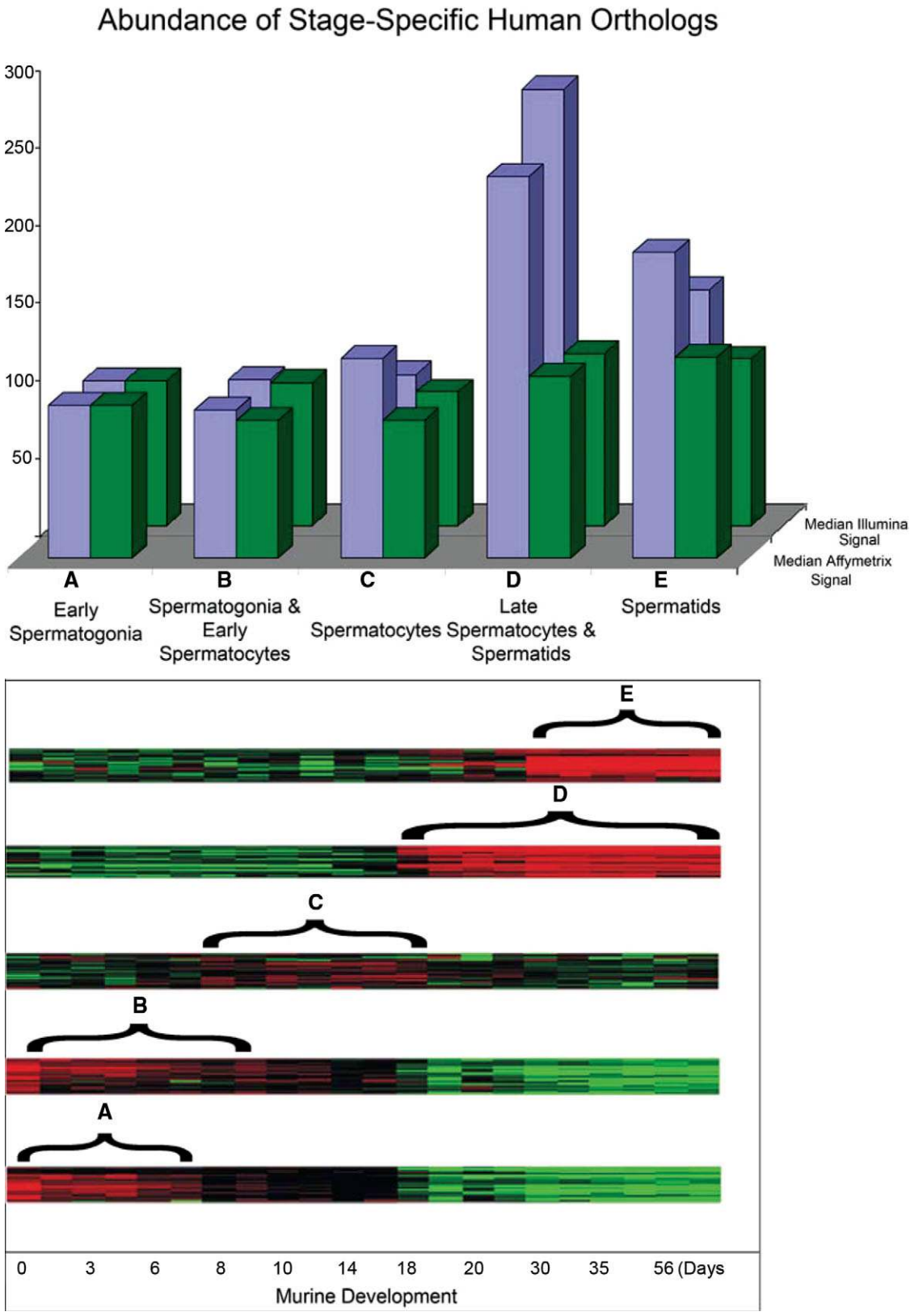

Figure 5. Disruption of spermatogenic gene expression during teratozoospermic development and differentiation. (**A**–**E**) Lower panel: heat maps of over 100 murine testes transcripts displaying germ cell type-specific expression (50). (**A**–**E**) Upper panel: relative abundance of the human orthologous RNAs identified from spermatozoal RNAs that were present within each cell type. The signal quantified from Ns (blue) and T_z teratozoospermic spermatozoal (green) profiles provides a silhouette to reveal a significant departure in the number of transcripts present from the late stage spermatocytes onward.

ontologically clustered. This clustering reiterated the ontology groups that were identified through the comparison of normalized expression profiles.

Transcript and sample clustering

Hierarchical clustering was performed using correlation as the distance metric and cluster centroids as the clustered elements in DChip for both the Affymetrix and Illumina data. Illumina data were imported as an external data set following normalization in BeadStudio. Clustering results were assessed for their stability relative to a similar clustering performed in the BeadStudio suite for the samples analyzed using the Illumina platform. Clustering of Affymetrix data utilized Cluster 3.0 and Java TreeView (44,45). Sample clustering was not sensitive to the analysis package. PCA was performed on data from the Affymetrix samples and Illumina samples in DChip using a subset of genes determined to be at least 10-fold different at $P < 0.001$ between the two groups. This was again replicated by PCA conducted in Cluster 3.0. The gene list of differentially expressed genes was then used to cluster an independent sample set shown in Figure 3. The significance of this perfect sample clustering in which all samples clustered with pathology at the level of the most significant bifurcation in a hierarchical cluster (centroids/correlation) was assessed as $P \simeq 0.015$ based on the generation of 300 random gene lists of the same size (the number required to stabilize the *P*-value) and the ability of these random gene lists to ideally cluster the independent sample set at the first bifurcation.

Ontological and pathway mapping of the differentially abundant transcripts from both the Illumina and Affymetrix platforms were undertaken using the NIH DAVID 2.1 system (12), Ariadne Genomics Pathway Studio (14) and Genomatix Bibliosphere (13). Transcripts not likely to be present in testes and germ cells but potentially arising elsewhere in the urogenital system that could be carried on the sperm surface (46) were considered. A tissue-specific transcriptional model was created for seminal vesicle and prostate using NCBI Gene Expression Omnibus (47) sample data sets: GSM44682 and GSM44678. The possible contribution to the ontologies and pathways arising from these tissues was then discounted from the analysis. This eliminated members of the oxidative phosphorylation and ribosome pathways from further consideration. The data were summarized relative to its assignment by NIH DAVID 2.1, referenced primarily with respect to the GO ontological annotations (48) and the KEGG pathway (30) databases.

Determination of transcripts with high stage specificity

Murine spermatogenesis proceeds over ~30 days. It provides a well-established developmental model that can be extrapolated to the 60-day human spermatogenic cycle to infer cell type specificity of human spermatozoal transcripts (49). The Gene Expression Omnibus (47), GEO series 926 (GSE926 URL: http://www.ncbi.nlm.nih.gov/geo/query/acc.cgi?acc = GSE926) was used to mine the developmental expression of genes during murine spermatogenesis. Cell type specific genes were derived from the hierarchical clustering of GEO data sets GDS605, GDS606 and GDS607, in which only those genes with a consistent pattern of high expression in one period of spermatogenesis and low expression in others were selected. Human orthologs were then identified using the NCBI's Homologene database system (27). At least 100 highly stage-specific transcripts that mapped to their human orthologs were identified. The relative abundance of transcripts present in sperm was used to assess the percentage of transcriptional signal expected to be provided by different spermatogenic cell types in N_s and T_z samples. In brief, the signal contributed by transcripts exhibiting high cell type specificity was gathered into signal bins. Binned signal levels were then used to assess the contribution at each cell type to the final profile observed in sperm. Differences between the N_s and T_z samples were then used to infer deviation from the normal spermatogenic pathway.

SUPPLEMENTARY MATERIAL

Supplementary Material is available at HMG Online.

ACKNOWLEDGEMENTS

The authors gratefully acknowledge the Michigan Economic Development Corporation, the Michigan Technology Tri-corridor program (Grant 085P4001419) and the Department of Obstetrics and Gynecology, Wayne State University, the CEGyR Foundation and grants from CONICET (PIP 2565) and ANPCyT (PICT 9591) for their support of this research program.

Conflict of Interest statement. We declare we have no conflict of interest.

Disclaimer. This work was reviewed by EPA and approved for publication but does not necessarily reflect official Agency policy. Mention of trade names or commercial products does not constitute endorsement or recommendation by EPA for use.

REFERENCES

1. Ostermeier, G.C., Dix, D.J., Miller, D., Khatri, P. and Krawetz, S.A. (2002) Spermatozoal RNA profiles of normal fertile men. *Lancet*, **360**, 772–777.
2. Lambard, S., Galeraud-Denis, I., Martin, G., Levy, R., Chocat, A. and Carreau, S. (2004) Analysis and significance of mRNA in human ejaculated sperm from normozoospermic donors: relationship to sperm motility and capacitation. *Mol. Hum. Reprod.*, **10**, 535–541.
3. Wang, H., Zhou, Z., Xu, M., Li, J., Xiao, J., Xu, Z.Y. and Sha, J. (2004) A spermatogenesis-related gene expression profile in human spermatozoa and its potential clinical applications. *J. Mol. Med.*, **82**, 317–324.
4. Krawetz, S.A. (2005) Paternal contribution: new insights and future challenges. *Nat. Rev. Genet.*, **6**, 633–642.
5. Rassoulzadegan, M., Grandjean, V., Gounon, P., Vincent, S., Gillot, I. and Cuzin, F. (2006) RNA-mediated non-mendelian inheritance of an epigenetic change in the mouse. *Nature*, **441**, 469–474.
6. Gur, Y. and Breitbart, H. (2006) Mammalian sperm translate nuclear-encoded proteins by mitochondrial-type ribosomes. *Genes Dev.*, **20**, 411–416.
7. Organization, W.H. (1993) *WHO Manual for the Standardised Investigation and Diagnosis of the Infertile Couple.*Cambridge University Press, Cambridge, UK.

8. Ombelet, W., Menkveld, R., Kruger, T.F. and Steeno, O. (1995) Sperm morphology assessment: historical review in relation to fertility. *Hum. Reprod. Update*, **1**, 543–557.
9. Chemes, E.H. and Rawe, Y.V. (2003) Sperm pathology: a step beyond descriptive morphology. Origin, characterization and fertility potential of abnormal sperm phenotypes in infertile men. *Hum. Reprod. Update*, **9**, 405–428.
10. Szczygiel, M. and Kurpisz, M. (1999) Teratozoospermia and its effect on male fertility potential. *Andrologia*, **31**, 63–75.
11. Van Waart, J., Kruger, T.F., Lombard, C.J. and Ombelet, W. (2001) Predictive value of normal sperm morphology in intrauterine insemination (IUI): a structured literature review. *Hum. Reprod. Update*, **7**, 495–500.
12. Dennis, G., Jr, Sherman, B.T., Hosack, D.A., Yang, J., Gao, W., Lane, H.C. and Lempicki, R.A. (2003) DAVID: Database for Annotation, Visualization, and Integrated Discovery. *Genome Biol.*, **4**, P3.
13. Dohr, S., Klingenhoff, A., Maier, H., Hrabe de Angelis, M., Werner, T. and Schneider, R. (2005) Linking disease-associated genes to regulatory networks via promoter organization. *Nucleic Acids Res.*, **33**, 864–872.
14. Nikitin, A., Egorov, S., Daraselia, N. and Mazo, I. (2003) Pathway studio–the analysis and navigation of molecular networks. *Bioinformatics*, **19**, 2155–2157.
15. Jervis, K.M. and Robaire, B. (2002) Changes in gene expression during aging in the Brown Norway rat epididymis. *Exp. Gerontol.*, **37**, 897–906.
16. Tengowski, M.W., Feng, D., Sutovsky, M. and Sutovsky, P. (2007) Differential expression of genes encoding constitutive and inducible 20S proteasomal core subunits in the testis and epididymis of theophylline- or 1,3-dinitrobenzene-exposed rats. *Biol. Reprod.*, **76**, 149–163.
17. Sutovsky, P., Manandhar, G., Laurincik, J., Letko, J., Caamano, J.N., Day, B.N., Lai, L., Prather, R.S., Sharpe-Timms, K.L., Zimmer, R. *et al*. (2005) Expression and proteasomal degradation of the major vault protein (MVP) in mammalian oocytes and zygotes. *Reproduction*, **129**, 269–282.
18. Coux, O., Tanaka, K. and Goldberg, A.L. (1996) Structure and functions of the 20S and 26S proteasomes. *Annu. Rev. Biochem.*, **65**, 801–847.
19. Hershko, A. and Ciechanover, A. (1998) The ubiquitin system. *Annu. Rev. Biochem.*, **67**, 425–479.
20. Haraguchi, C.M., Mabuchi, T., Hirata, S., Shoda, T., Hoshi, K. and Yokota, S. (2004) Ubiquitin signals in the developing acrosome during spermatogenesis of rat testis: an immunoelectron microscopic study. *J. Histochem. Cytochem.*, **52**, 1393–1403.
21. Sutovsky, P. (2003) Ubiquitin-dependent proteolysis in mammalian spermatogenesis, fertilization, and sperm quality control: killing three birds with one stone. *Microsc. Res. Tech.*, **61**, 88–102.
22. Lin, H., Yin, L., Reid, J., Wilkinson, K.D. and Wing, S.S. (2001) Divergent N-terminal sequences of a deubiquitinating enzyme modulate substrate specificity. *J. Biol. Chem.*, **276**, 20357–20363.
23. Sutovsky, P., Moreno, R., Ramalho-Santos, J., Dominko, T., Thompson, W.E. and Schatten, G. (2001) A putative, ubiquitin-dependent mechanism for the recognition and elimination of defective spermatozoa in the mammalian epididymis. *J. Cell Sci.*, **114**, 1665–1675.
24. Sutovsky, P., Terada, Y. and Schatten, G. (2001) Ubiquitin-based sperm assay for the diagnosis of male factor infertility. *Hum. Reprod.*, **16**, 250–258.
25. Ginalski, K., Rychlewski, L., Baker, D. and Grishin, N.V. (2004) Protein structure prediction for the male-specific region of the human Y chromosome. *Proc. Natl. Acad. Sci. USA*, **101**, 2305–2310.
26. Tse, J.Y., Wong, E.Y., Cheung, A.N., O, W.S., Tam, P.C. and Yeung, W.S. (2003) Specific expression of VCY2 in human male germ cells and its involvement in the pathogenesis of male infertility. *Biol. Reprod.*, **69**, 746–751.
27. Wheeler, D.L., Barrett, T., Benson, D.A., Bryant, S.H., Canese, K., Chetvernin, V., Church, D.M., DiCuccio, M., Edgar, R., Federhen, S. *et al*. (2006) Database resources of the National Center for Biotechnology Information. *Nucleic Acids Res.*, **34**, D173–D180.
28. Dix, D.J., Allen, J.W., Collins, B.W., Poorman-Allen, P., Mori, C., Blizard, D.R., Brown, P.R., Goulding, E.H., Strong, B.D. and Eddy, E.M. (1997) HSP70–2 is required for desynapsis of synaptonemal complexes during meiotic prophase in juvenile and adult mouse spermatocytes. *Development (Cambridge, England)*, **124**, 4595–4603.
29. Cao, W., Gerton, G.L. and Moss, S.B. (2006) Proteomic profiling of accessory structures from the mouse sperm flagellum. *Mol. Cell. Proteomics*, **5**, 801–810.
30. Kanehisa, M. and Goto, S. (2000) KEGG: kyoto encyclopedia of genes and genomes. *Nucleic Acids Res.*, **28**, 27–30.
31. Richert, L., Liguori, M., Abadie, C., Heyd, B., Mantion, G., Halkic, N. and Waring, J. (2006) Gene expression in human hepatocytes in suspension after isolation is similar to the liver of origin, is not affected by hepatocyte cold storage and cryopreservation, but is strongly changed after hepatocyte plating. *Drug Metab. Disp.*, **34**, 870–879.
32. Mizushima, N., Yamamoto, A., Matsui, M., Yoshimori, T. and Ohsumi, Y. (2004) *In vivo* analysis of autophagy in response to nutrient starvation using transgenic mice expressing a fluorescent autophagosome marker. *Mol. Biol. Cell*, **15**, 1101–1111.
33. Wojcik, C., Benchaib, M., Lornage, J., Czyba, J.C. and Guerin, J.F. (2000) Proteasomes in human spermatozoa. *Int J Androl*, **23**, 169–177.
34. Ostermeier, G.C., Goodrich, R.J., Diamond, M.P., Dix, D.J. and Krawetz, S.A. (2005) Toward using stable spermatozoal RNAs for prognostic assessment of male factor fertility. *Fertil. Steril.*, **83**, 1687–1694.
35. Golub, T.R., Slonim, D.K., Tamayo, P., Huard, C., Gaasenbeek, M., Mesirov, J.P., Coller, H., Loh, M.L., Downing, J.R., Caligiuri, M.A. *et al*. (1999) Molecular classification of cancer: class discovery and class prediction by gene expression monitoring. *Science*, **286**, 531–537.
36. Oliphant, A., Barker, D.L., Stuelpnagel, J.R. and Chee, M.S. (2002) BeadArray technology: enabling an accurate, cost-effective approach to high-throughput genotyping. *Biotechniques*, **32**: (suppl.) 56–61.
37. Platts, A., Dix, D.J. and Krawetz, S.A. (2006) Considerations when using Array Technologies for male factor assessment. *Genetics of Male Infertility*, Humana Press. Totowa, New Jersey.
38. Liu, W.M., Mei, R., Di, X., Ryder, T.B., Hubbell, E., Dee, S., Webster, T.A., Harrington, C.A., Ho, M.H., Baid, J. *et al*. (2002) Analysis of high density expression microarrays with signed-rank call algorithms. *Bioinformatics*, **18**, 1593–1599.
39. Li, C. and Wong, W.H. (2001) Model-based analysis of oligonucleotide arrays: expression index computation and outlier detection. *Proc. Natl Acad. Sci. USA*, **98**, 31–36.
40. Larsson, O., Wahlestedt, C. and Timmons, J.A. (2005) Considerations when using the significance analysis of microarrays (SAM) algorithm. *BMC Bioinformatics*, **6**, 129.
41. Irizarry, R.A., Bolstad, B.M., Collin, F., Cope, L.M., Hobbs, B. and Speed, T.P. (2003) Summaries of Affymetrix GeneChip probe level data. *Nucleic Acids Res.*, **31**, e15.
42. Lee, M.L. and Whitmore, G.A. (2002) Power and sample size for DNA microarray studies. *Stat. Med.*, **21**, 3543–3570.
43. Illumina (BeadStudio), http://www.illumina.com.2007.
44. Eisen, M.B., Spellman, P.T., Brown, P.O. and Botstein, D. (1998) Cluster analysis and display of genome-wide expression patterns. *Proc. Natl Acad. Sci. USA*, **95**, 14863–14868.
45. Saldanha, A.J. (2004) Java Treeview—extensible visualization of microarray data. *Bioinformatics*, **20**, 3246–3248.
46. Bjartell, A., Malm, J., Moller, C., Gunnarsson, M., Lundwall, A. and Lilja, H. (1996) Distribution and tissue expression of semenogelin I and II in man as demonstrated by *in situ* hybridization and immunocytochemistry. *J. Androl.*, **17**, 17–26.
47. Barrett, T., Suzek, T.O., Troup, D.B., Wilhite, S.E., Ngau, W.C., Ledoux, P., Rudnev, D., Lash, A.E., Fujibuchi, W. and Edgar, R. (2005) NCBI GEO: mining millions of expression profiles—database and tools. *Nucleic Acids Res.*, **33**, D562–D566.
48. Camon, E., Magrane, M., Barrell, D., Binns, D., Fleischmann, W., Kersey, P., Mulder, N., Oinn, T., Maslen, J., Cox, A. *et al*. (2003) The Gene Ontology Annotation (GOA) project: implementation of GO in SWISS-PROT, TrEMBL, and InterPro. *Genome Res.*, **13**, 662–672.
49. Martins, R.P. and Krawetz, S.A. (2005) RNA in human sperm. *Asian J. Androl.*, **7**, 115–120.
50. Shima, J.E., McLean, D.J., McCarrey, J.R. and Griswold, M.D. (2004) The murine testicular transcriptome: characterizing gene expression in the testis during the progression of spermatogenesis. *Biol. Reprod.*, **71**, 319–330.